

## Acid–base properties of Mg–Ni–Al mixed oxides using LDH as precursors

S. Casenave<sup>a</sup>, H. Martinez<sup>a</sup>, C. Guimon<sup>a,\*</sup>, A. Auroux<sup>b</sup>,  
V. Hulea<sup>c</sup>, A. Cordoneanu<sup>c</sup>, E. Dumitriu<sup>c</sup>

<sup>a</sup>LPCM–UMR (CNRS) 5624, 2 Avenue P. Angot, 64053 Pau Cedex 09, France

<sup>b</sup>IRC, 2 Avenue A. Einstein, 69626 Villeurbanne Cedex, France

<sup>c</sup>Laboratory of Catalysis, Technical University of Iasi, 71 D. Mangeron, Iasi, Romania

### Abstract

The thermal behavior of a series of Mg/Ni/Al hydrotalcites with (Mg + Ni)/Al = 2 and different Mg/Ni ratios has been studied (by means of X-ray diffraction (XRD), thermogravimetry and X-ray photoelectron spectroscopy (XPS), as well as the acid–base properties of the mixed oxides resulting from their calcination at 723 K (by means of adsorption microcalorimetry).

Up to 500 K, only the physisorbed and interlayer water is released, causing a small loss of crystallinity. The decomposition of carbonate anions begins above 500 K, but this loss does not destroy the LDH structure which remains up to temperatures between 600 and 650 K. Above, the structure collapses and dehydroxylation occurs, leading to the formation of mixed oxides with large surface areas. At 723 K, a temperature usually chosen for the catalytic reactions, about 30% of the initial carbonates are still detected and poison a part of the strongest basic sites. The decarbonation is practically completed at 923 K. When the stability of the carbonates increases with the nickel content, the stability of the hydroxides increases, on the contrary, with the magnesium content.

The NH<sub>3</sub> adsorption data indicate an increase of the concentration and strength of acid sites with the nickel content. The compound SO<sub>2</sub> seems to be more efficient than CO<sub>2</sub> for the analysis of the basicity, because of its higher acidity and the presence of remaining carbonates in the mixed oxides. The highest concentration of basic sites is observed for the Mg/Ni/Al sample with low magnesium and high nickel contents. This gives evidence of the synergy effect of these metals favoring the basic properties and the role of MgO as promoter. Above 723 K, the concentration of the basic sites of mixed oxides decreases, which can be related to a more complete dehydroxylation. © 2001 Elsevier Science B.V. All rights reserved.

**Keywords:** Mg–Ni–Al mixed oxides; Dehydroxylation; Precursors

### 1. Introduction

Hydrotalcites or layered double hydroxides (LDHs) [1] belong to a large class of natural and synthetic anionic clays. They are less diffuse in nature than

cationic clays, but they can be easily synthesized. Hydrotalcite-type compounds have the general formula:  $[M_{1-x}^{2+}M_x^{3+}(\text{OH})_2]^{x+}[A_{x/n}^{n-}]_m \cdot m\text{H}_2\text{O}$ , where  $M^{2+} = \text{Mg}^{2+}, \text{Ni}^{2+}, \text{Zn}^{2+}, \dots; M^{3+} = \text{Al}^{3+}, \text{Fe}^{3+}, \dots; A = \text{anion}$  (usually carbonate). Their structure is similar to that of the brucite  $\text{Mg}(\text{OH})_2$  where octahedra of  $\text{Mg}^{2+}$  (six-fold coordinated to  $\text{OH}^-$ ) share edges to form infinite sheets. These latter are stacked on top of each other and are held together by hydrogen bonding. When  $\text{Mg}^{2+}$  is substituted by a trivalent

\* Corresponding author. Tel.: +33-55-984-3150;

fax: +33-559-808-344.

E-mail address: [claud.guimon@univ-pau.fr](mailto:claud.guimon@univ-pau.fr) (C. Guimon).

cation (with a radius close to that of  $\text{Mg}^{2+}$ ), a formal positive charge appears in hydroxyl layers. The electroneutrality and the stability are assured by anions  $\text{A}^{n-}$  and water which are located in the interlayer region. Commonly,  $x$  is in the range 0.2–0.33 ( $\text{M}^{2+}/\text{M}^{3+}$  between 2 and 4).

These compounds have many industrial applications, particularly in basic catalysis, either as such or after controlled thermal decomposition. Thermal treatments induce dehydration, dehydroxylation and loss of compensating anions, and lead to basic mixed oxides with a high surface area, a homogeneous interdispersion of the metals and a better resistance to sintering than corresponding supported catalysts. The activity of these catalysts, related to their acid–base and/or redox (when they contain a reducible metal) properties, depends on their composition, the preparation method and the treatment conditions.

In the first part of this work, we examine the thermal decomposition of LDHs by XRD, TGA and X-ray photoelectron spectroscopy (XPS); in a second part, we determine the influence of the composition of Mg–Ni–Al mixed oxides obtained by calcination at 723 K of a series of hydrotalcites (with  $\text{M}^{2+}/\text{M}^{3+} = 2$ , Ni/Mg ratio varying from 0 to  $\infty$ , carbonate as compensating anion) on their acid and base properties, with the help of adsorption microcalorimetry.

## 2. Experimental

### 2.1. Materials

Hydrotalcite compounds (LDHs) with different Mg/Ni/Al molar ratios were elaborated by precipitation under low supersaturation, wherein both the precipitants ( $\text{NaOH}$  and  $\text{Na}_2\text{CO}_3$ ) and the corresponding metal nitrates were added slowly, while the pH was held constant. The precipitate was hydro-thermally treated in a Teflon-coated autoclave at 453 K for 12 h. The resulting solid was isolated, washed with deionized water and dried overnight at 353 K.

The samples are named according to their formal composition: Mg/Ni/Al 2/0/1, 1.67/0.33/1, 1.33/0.67/1, 1/1/1, 0.67/1.33/1, 0.33/1.67/1 and 0/2/1. The real compositions, determined by ICP AES, are very close to these ones.

### 2.2. Characterization

The X-ray diffraction (XRD) patterns were recorded on an INEL diffractometer using a curved position-sensitive detector (INEL CPS 120) calibrated with  $\text{Na}_2\text{Ca}_3\text{Al}_2\text{F}_{14}$  as standard. The monochromatized radiation applied was  $\text{Cu K}\alpha$  (1.5406 Å) from a long fine focus Cu tube operating at 40 kV and 35 mA. Scans were performed over the  $2\theta$  range from 5 to  $115^\circ$ . Accurate unit cell parameters were determined by a least-squares refinement from data collected by the diffractometer.

Thermogravimetric experiments were carried out on a TGA model 2950 (TA Instruments) using about 5 mg of sample, from 313 to 873 K ( $4 \text{ K min}^{-1}$ ), under a nitrogen flow.

The XPS analyses were performed at room temperature with a SSI spectrometer using a monochromatic and focused (spot diameter of 600  $\mu\text{m}$ , 100 W) Al  $\text{K}\alpha$  radiation (1486.6 eV) under a residual pressure of  $5 \times 10^{-8}$  Pa. The introduction chamber of the spectrometer was coupled with a glove-box for the analysis of the calcined samples. Charge effects were compensated by the use of a flood gun (5 eV). The hemispherical analyzer functioned with a constant pass energy of 50 eV for high resolution spectra. The experimental bands were fitted with theoretical bands (80% Gaussian, 20% Lorentzian) with a least-squares algorithm using non-linear baseline.

The heats of adsorption were measured in a heat flow microcalorimeter of the Tian–Calvet type (C80 from Setaram), linked to a volumetric line allowing the introduction of small doses of reactive gaseous probes ( $\text{NH}_3$ ,  $\text{CO}_2$ ,  $\text{SO}_2$ ). The equilibrium pressure after each introduction of gas was measured by means of a differential pressure gauge from datametrics. Successive doses were sent onto the sample until a final equilibrium pressure of 67 Pa was obtained. Before adsorption, samples were outgassed at 723 K overnight; the adsorption was performed at 353 K in order to limit physisorption. The amount of intermediate and strong sites was evaluated from the difference between the primary and the secondary isotherms obtained after desorption under secondary vacuum ( $10^{-4}$  Pa) at 353 K and readsorption of the gas under an equilibrium pressure of 27 Pa. This difference is named irreversibly chemisorbed amount ( $V_{\text{irr}}$ ).

### 3. Results and discussion

#### 3.1. Thermal decomposition of hydrotalcites

The characteristics of the hydrotalcites, following the different stages of calcination, are very important because they determine their catalytic properties, and particularly the acid–base properties. The thermal evolution of the LDH structure can be easily studied by classical techniques such as XRD and thermogravimetry analysis (TGA). Moreover, the loss of the carbonate anions, located near the surface of the crystallites, can be evaluated as a function of the calcination temperature by XPS.

The XRD pattern (Fig. 1a) for a representative LDH (Mg/Ni/Al: 1/1/1) exhibits sharp and symmetric reflections for (0 0 3), (0 0 6), (1 1 0) and (1 1 3) planes and broad and asymmetric reflections for (1 0 2), (1 0 5) and (1 0 8) planes, characteristic of some common features of this kind of well crystallized layered compounds. The classical rhombohedral 3R stacking symmetry is found. The parameters of the unit cell are  $a$  ( $2 \times d_{110}$ , with respect to hexagonal

axes) and  $c = 3 \times c'$ , where  $c'$  is the thickness of one layer constituted by a brucite-like sheet and one interlayer. No excess phase was detected, suggesting that  $\text{Ni}^{2+}$  has isomorphically replaced the  $\text{Mg}^{2+}$  cations in the brucite layers.

From the position of the strongest lines, of crystallographic indices (0 0 3) and (1 1 0), the lattice distances  $d_{003}$  and  $d_{110}$  were calculated and used to determine the lattice parameters  $c$  ( $3 \times d_{003} = 22.483 \text{ \AA}$ ) and  $a$  ( $2 \times d_{110} = 2.980 \text{ \AA}$ ). These values are close to those of the literature for this type of material [2].

The LDH samples were calcined under inert gas, over the temperature range 273–923 K and then analyzed by XRD. The corresponding spectra are presented in Fig. 1b–f. There are two temperature regions which are distinguished by the XRD pattern,  $273 \text{ K} \leq T \leq 573 \text{ K}$  and  $573 \text{ K} \leq T \leq 923 \text{ K}$ .

Sharp and intense lines are observed in the first temperature region. The sample still displays typical LDH structure (Fig. 1b and c). The (0 0 3) and (0 0 6) reflections are observed until 573 K. However, the (0 0 1) peaks are clearly broadened as the temperature increases, suggesting a disorder in the layers stacking and a loss of the crystalline order. The usual decrease in basal spacing [3,4] due to the loss of interlayer water and carbonates from the LDH could not be observed in any obvious manner for this compound. This is not an artefact and could be accounted by a different orientation of carbonate anions, as proposed by Tichit et al. [5], and maybe a partial rehydration due to the recording time (3 h) of diffraction spectra in atmosphere. Furthermore, around 573 K the (1 1 0) lines are modified as the temperature increases.

It should be noted, in the XRD patterns recorded at 573 and 673 K, the presence of a reflection at  $d = 0.227 \text{ nm}$  which does not belong to a mixed oxide structure and could not be attributed unambiguously to a specific specie or structure. This reflection could be assigned to the presence of an impurity, present in the MgNiAl LDH. This impurity could crystallize in the temperature range around 573 K and disappear at 723 K.

The crystallographic transition from the layered structure to a mixed oxide structure takes place over 573 K. The two phases are not simultaneously observed. The (0 0 1) reflections all vanish, and the spectra 1d–f present only a broad series corresponding

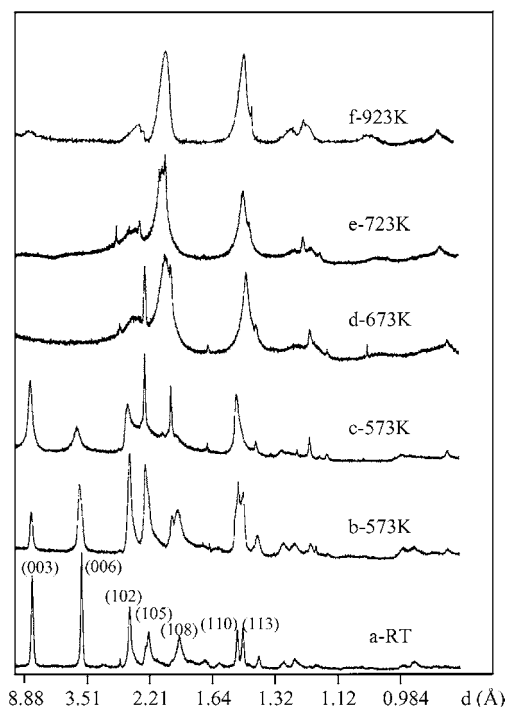


Fig. 1.

to reflections close to those of periclase MgO (JCPDS file no. 43–1022) and/or NiO (JCPDS file no. 22–1189), in agreement with the literature [6,7], in addition to amorphous aluminum oxide.

The most striking feature of the pattern after calcination above 573 K is the conversion of the LDH to an amorphous oxide material, after dehydration, dehydroxylation and loss of the charge compensating anions.

This result is confirmed by the thermogravimetric analyses. In Fig. 2, are reported the TG/DTG curves (weight losses as a function of temperature and the

corresponding differential curves) of Mg/Ni/Al 2/0/1, 1/1/1 and 0/2/1 LDH samples. The total weight loss is about 38% for Mg–Al LDH (2/0/1) and in the range 29–31% for the other samples. As already observed [5], this difference can be related to the higher affinity of water for magnesium compared to nickel.

The low temperature weight loss, which occurs at about 460 K, is attributed to the removal of physisorbed and interlayer water. As observed by XRD, the hydroxalcite structure remains, which can be explained by the results of Reichle et al. [8]: water and, later, carbon dioxide are released by a cratering mechanism

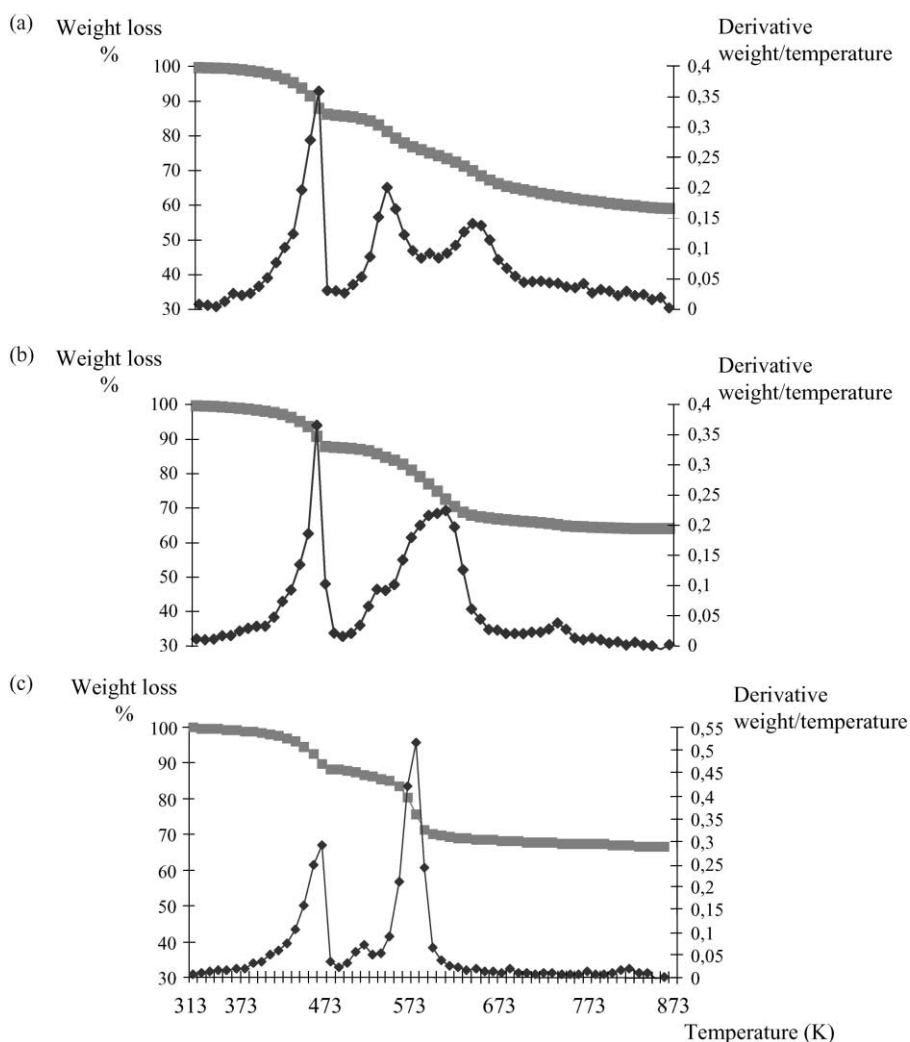


Fig. 2.

rather than by exfoliation. This induces a microporosity of the samples, with narrow pore size distribution [2], and a considerable increase of their BET specific area (from about  $50 \text{ m}^2 \text{ g}^{-1}$  at RT to  $250 \text{ m}^2 \text{ g}^{-1}$  after calcination). Above 500 K, loss of  $\text{CO}_2$ , from decomposition of carbonates, and water, from dehydroxylation, occurs. In agreement with Rey et al. [3], two steps are observed, at least for Mg–Al LDH (2/0/1). The first one at about 545 K can be attributed to the beginning of dehydroxylation and to the elimination of a part of the carbonate ions. This is confirmed by the XPS analyses. The XP C 1s spectra recorded at increasing temperatures (Fig. 3), show the elimination of carbonate ions (peak at about 289 eV, the low binding energy band at 284.6 eV, coming from the surface adventitious carbon). This elimination of  $\text{CO}_3^{2-}$  as a function of temperature is quantified in Fig. 4 (the

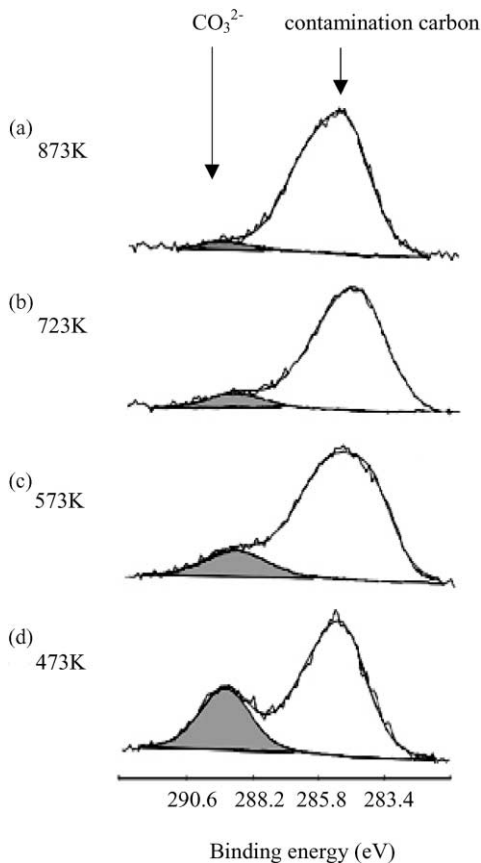


Fig. 3.

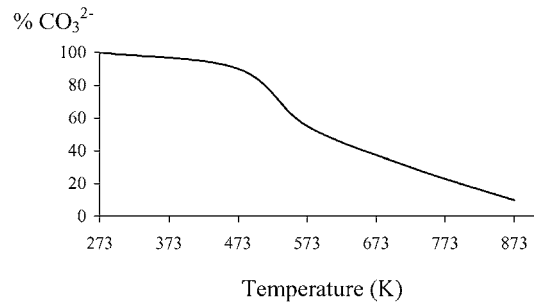


Fig. 4.

0.33/1.67/1 sample is taken for example, but all the samples show the same evolution). It begins at about 473 K. Half of the initial carbonates are eliminated at 573 K, though the LDH structure still remains at this temperature (Fig. 1). At 723 K, the usual calcination temperature for hydrotalcites, about 30% of the initial  $\text{CO}_3^{2-}$  are detected on the surface of the mixed oxides. This could come from a readsorption of  $\text{CO}_2$  on the strong basic sites  $\text{O}^{2-}$  of the oxides. The second step, around 640 K, corresponds to the continuation of the decarbonation and the dehydroxylation, i.e. to the transformation of the hydroxides into oxides, which causes a collapse of the structure.

For the Mg-rich LDH, the second step occurs at higher temperature than for Ni-rich ones. This can be attributed to a stronger basic character of the former hydroxides and a better thermal stability.

#### 4. Acid–base character of mixed oxides

Adsorption microcalorimetry is a powerful technique for the characterization of acidic or basic properties of catalysts [9–11]. The acidic character of solids is usually studied with nitrogen basic probes, particularly ammonia [12]. The basic properties are often analyzed using  $\text{CO}_2$  as acid probe [13]. However, in the case of LDH containing carbonate anions which partly remain after calcination, the adsorption of sulfur dioxide is more suitable to study basic sites. The study of the acido–basicity concerns the LDH samples activated at 723 K, with the aim to perform further catalytic applications. Indeed, this temperature seems a good compromise since it gives stable mixed oxides with high specific surface areas

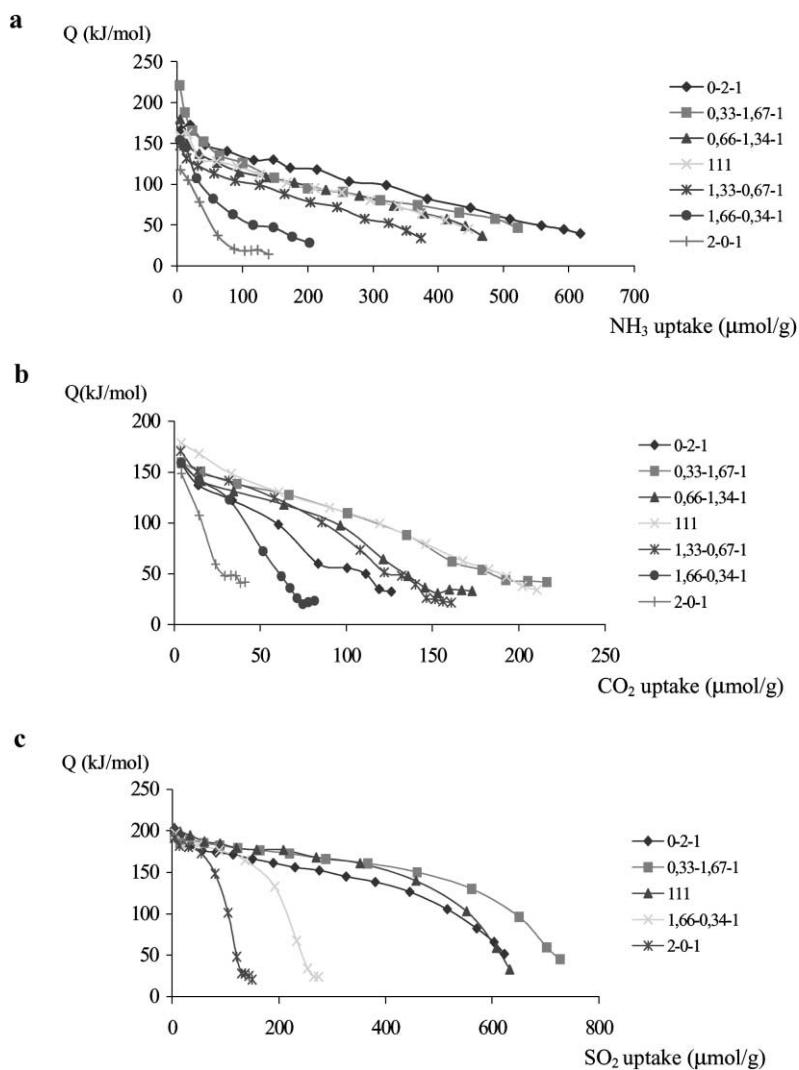


Fig. 5.

although a part of the strong basic sites is still blocked by remaining  $\text{CO}_2$ .

#### 4.1. Acidity

The differential heats of  $\text{NH}_3$  adsorption as a function of the ammonia uptake for the calcined hydroxal-cites are reported in Fig. 5a. In our experimental conditions, two types of behavior of the adsorption heat versus coverage appear. Higher initial adsorption heats are obtained for the Ni-rich oxides (150–

180  $\text{kJ mol}^{-1}$ ). The sample 0.33/1.67/1 presents the strongest sites. The curves slowly decrease to 70  $\text{kJ mol}^{-1}$  — value usually considered as the chemisorption-physisorption limit — with the exception of the samples containing high amounts of magnesium which show only few acid sites. As shown by XPS (analysis after  $\text{NH}_3$  adsorption as previously described [14]), they are Lewis sites. The amount of medium and strong acid sites, measured by the  $\text{NH}_3$  volume irreversibly adsorbed ( $V_{\text{irr}}$ ), follows the nickel content (Table 1).

Table 1  
Irreversibly chemisorbed CO<sub>2</sub>, SO<sub>2</sub> and NH<sub>3</sub> amounts (μmol g<sup>-1</sup>) at 353 K

	V <sub>irr</sub>		
	CO <sub>2</sub>	SO <sub>2</sub>	NH <sub>3</sub>
Mg/Ni/Al (0/2/1)	71.5	490	343
Mg/Ni/Al (0.33/1.67/1)	149.5	619	278.5
Mg/Ni/Al (0.66/1.33/1)	115		220
Mg/Ni/Al (1/1/1)	143	543	200
Mg/Ni/Al (1.33/0.67/1)	116.5		155
Mg/Ni/Al (1.67/0.33/1)	60	242	62.5
Mg/Ni/Al (2/0/1)	21.5	120	54.5

#### 4.2. Basicity

Fig. 5b and c show the differential heats of adsorption of acid probe molecules, CO<sub>2</sub> and SO<sub>2</sub>,

respectively, versus coverage. The initial adsorption heats of SO<sub>2</sub> are higher by about 20 kJ mol<sup>-1</sup> than that of CO<sub>2</sub>. The compound SO<sub>2</sub> seems to be more efficient than CO<sub>2</sub> to probe the basicity. Indeed, at the chosen activation temperature (723 K), as revealed by XPS analysis, about 30% of carbonates remain inside the sample, which disturbs the measurement of the basicity by CO<sub>2</sub>. The compound SO<sub>2</sub>, which is a stronger acid than CO<sub>2</sub>, displaces it partly (about the half of remaining CO<sub>2</sub> has disappeared after adsorption of SO<sub>2</sub>). Then the presence of strong basic sites is better detected by SO<sub>2</sub> than by CO<sub>2</sub>. The evolution of the adsorption over the basic sites as a function of the Mg/Ni/Al composition is similar for the two probe molecules. However, the number of covered basic sites is clearly more important with SO<sub>2</sub> than CO<sub>2</sub>, which is related to the respective strengths of the two acids.

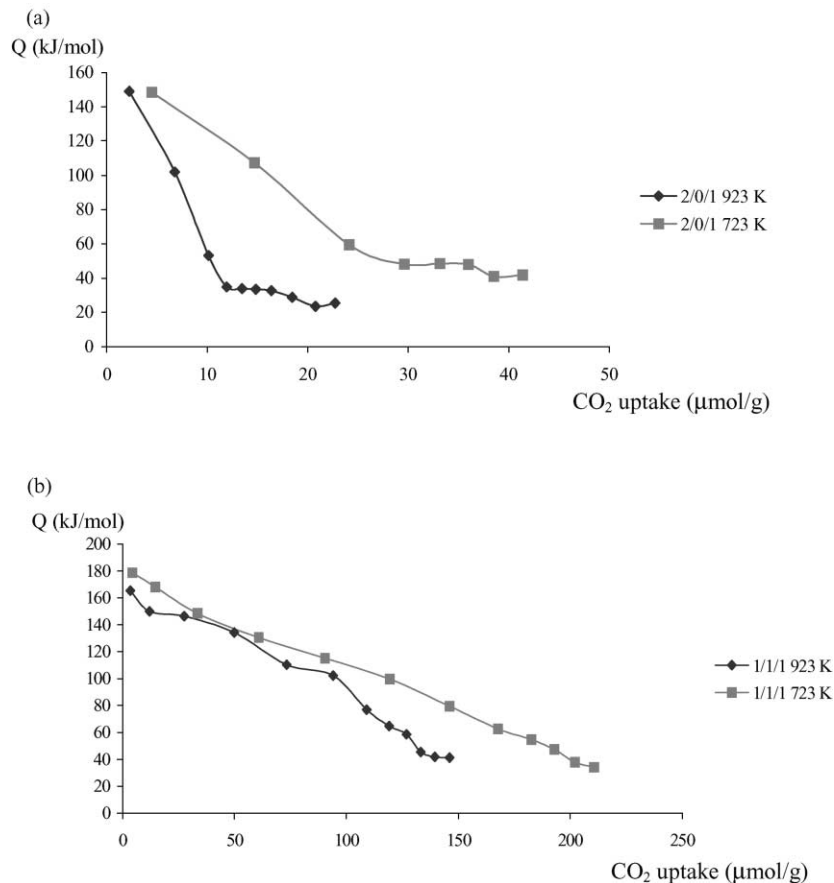


Fig. 6.

Table 2  
Irreversibly chemisorbed CO<sub>2</sub> amounts (μmol g<sup>-1</sup>) at 353 K after calcination at 723 and 923 K

	Mg/Ni/Al (2/0/1)		Mg/Ni/Al (1/1/1)	
	723	923	723	923
Activation temperature (K)	237	923	723	923
V <sub>irr</sub> (CO <sub>2</sub> ) (μmol g <sup>-1</sup> )	21.5	10	143	92.5

For sample Mg/Ni/Al 0/2/1, the heats in the range 150–200 kJ mol<sup>-1</sup>, are associated with a volume of 8 μmol g<sup>-1</sup> of CO<sub>2</sub> and 282 μmol g<sup>-1</sup> with SO<sub>2</sub>. This observation confirms the fact that carbonates, still present after calcination, occupy strong basic sites which are no more accessible for CO<sub>2</sub>. The adsorption of SO<sub>2</sub> proves that the strength of sites is linked with the proportion of magnesium and nickel. The presence of these two cations increases the concentration of basic sites. As shown in Table 1, the irreversibly adsorbed volume — corresponding to the medium and strong basic sites — is larger when Mg<sup>2+</sup> (in low concentration) and Ni<sup>2+</sup> (in large concentration) coexist. This study gives evidence of the synergetic effect of these two cations for the basic properties, MgO being a promoter of the Ni–Al system.

Fig. 6 and Table 2 report the influence of the calcination temperature on the basicity of mixed oxides, as measured by CO<sub>2</sub> adsorption calorimetry. Two temperatures are tested: 723 and 923 K for the two oxides Mg/Ni/Al, 2/0/1 and 1/1/1. The samples calcined at 723 K have more basic sites than those calcined at 923 K. This could be explained by a decrease of specific area and also by an incomplete dehydroxylation at 723 K, but not by the formation of spinel phase, as shown by XRD. The remaining OH basic groups at this temperature seem to correspond to relatively weak sites. This difference is more important when the sample is rich in magnesium. This is coherent with the better thermal stability (at 723 K) of magnesium hydroxide shown by the TG experiments (Fig. 2).

## 5. Conclusion

In this work, the thermal evolution of Mg/Ni/Al hydroxalicates has been studied, as well as the acid–base properties of the oxides resulting from their calcination at 723 K.

Up to 500 K, only the physisorbed and interlayer water is released, causing a small loss of crystallinity. Carbonate anions begin to be decomposed above 500 K, but this loss does not destroy the LDH structure which remains up to a temperature between 600 and 650 K. Above this temperature, the structure collapses and dehydroxylation occurs, inducing the formation of mixed oxides with large surface areas. At 723 K, a temperature usually chosen for catalytic reactions, about 30% of the initial carbonates are still detected on the surface, and hide a part of the strongest basic sites. The decarbonation is practically complete at 923 K. While the stability of the carbonates increases with the nickel content, the stability of the hydroxides increases with the magnesium content.

The adsorption data indicate an increase of the concentration and strength of acid sites with the nickel content. For the characterization of the basicity, SO<sub>2</sub> seems to be more efficient than CO<sub>2</sub> because of its higher acidity and the presence of remaining carbonates (according to the XPS data, SO<sub>2</sub> replaces about the half of the remaining CO<sub>2</sub>). The highest concentration of basic sites is observed for the Mg/Ni/Al sample with low magnesium and high nickel contents (0.33/1.67/1). This is evidence of the synergetic effect of these two cations favoring the basic properties.

Finally, the influence of the calcination temperature on the basicity of LDHs has been examined. The sensible difference in the CO<sub>2</sub> adsorption curves between the samples activated at 723 and 923 K indicates a real evolution in the properties of the calcined catalysts. A decrease of the specific areas and the hydroxide ions still present in the structure after a treatment at 723 K but absent at 923 K could explain a larger population of basic sites at the former temperature. However, these sites seem to be relatively weak.

## References

- [1] F. Cavani, F. Trifirò, A. Vaccari, *Catal. Today* 11 (1991) 173.
- [2] G. Forsanari, M. Gazzano, D. Matteuzzi, F. Trifirò, A. Vaccari, *Appl. Clay Sci.* 10 (1995) 69.
- [3] F. Rey, V. Fornés, J.M. Rojo, *J. Chem. Soc., Faraday Trans.* 88 (1992) 2233.
- [4] M.J. Hudson, S. Carlino, D.C. Apperley, *J. Mater. Chem.* 5 (1995) 323.
- [5] D. Tichit, F. Medina, B. Coq, R. Dutartre, *Appl. Catal A: Gen.* 159 (1997) 241.



- [6] O. Clause, M.G. Coelho, M. Gazzano, D. Matteuzzi, F. Trifirò, A. Vaccari, *Appl. Clay Sci.* 8 (1993) 169.
- [7] M.A. Aramendia, Y. Avilés, V. Borau, J.M. Luque, J.M. Marinas, J.R. Ruiz, F.J. Urbano, *J. Mater. Chem.* 9 (1999) 1603.
- [8] W.T. Reichle, S.Y. Kang, D.S. Everhardt, *J. Catal.* 101 (1986) 352.
- [9] A. Auroux, in: B. Imelik, J.C. Vedrine (Eds), *Les techniques physiques d'étude des catalyseurs*, Technip, Paris, 1988, p. 823.
- [10] N. Cardona-Martinez, J.A. Dumesic, *Advances in Catalysis*, Academic Press, New York, 1992, p. 38.
- [11] V. Solinas, I. Ferino, *Catal. Today* 41 (1998) 179.
- [12] A. Auroux, *Topics Catal.* 4 (1997) 71.
- [13] D. Tichit, M.H. Lhouty, A. Guida, B.H. Chiche, F. Figueras, A. Auroux, D. Bartalini, E. Garrone, *J. Catal.* 151 (1995) 50.
- [14] A. Boreave, A. Auroux, C. Guimon, *Micropor. Mater.* 11 (1997) 275.